Effect of destabilization heat treatment on the microstructure and wear properties of ASTM A532 high-chromium white cast iron

Sharada Prasad Shukla[1] , Sujith Bobba[2*], Mukkollu Sambasiva Rao[1*], Kamlesh Kumar Singh[3], Amitesh Kumar[3]

[1*]Research Scholar, NIAMT Ranchi, India

[2]Assistant Professor, Department of Mechanical Engineering, VNR Vignana Jyothi Instituteof Engineering and Technology Hyderabad, India

[3]Professor, NIAMT Ranchi, India

***samba.siva129@gmail.com & *sujith_b@vnrvjiet.in**

(Received 04 April 2026; Accepted 08 July 2026)

ABSTRACT

This study investigates the effect of molybdenum (Mo) content on the microstructure, hardness, and wear resistance of ASTM A532 eutectic high-chromium white cast iron (HCCI) subjected to destabilization heat treatment with different cooling paths. Three alloys containing 1.23%, 1.395%, and 1.86% Mo were destabilized at 995 °C and held for sufficient soaking time to promote secondary carbide precipitation and matrix transformation. After heat treatment, the specimens were subjected to several cooling routes, including still-air cooling, furnace cooling, oil quenching, and water quenching, to evaluate the influence of cooling rate on the resulting microstructure and wear behavior. Following cooling, all specimens were tempered at 400 °C to relieve residual stresses and stabilize the martensitic matrix. Microstructural analysis revealed that increasing Mo content promoted fine secondary carbide precipitation and improved matrix hardenability, while the cooling path significantly affected carbide distribution and martensite formation. Faster cooling paths such as oil and water quenching enhanced martensitic transformation and hardness, whereas slower cooling produced comparatively softer matrices with coarser carbides. Excessive Mo addition increased the fraction of primary M_7C_3 carbides at the expense of martensite formation. Abrasion testing according to ASTM G65-16 demonstrated that the alloy containing 1.86% Mo exhibited the best wear resistance, with a minimum volume loss of 9.03 mm^3, due to the combined effect of a high primary carbide fraction (40.72%) and dense secondary carbide precipitation. In contrast, the medium-Mo alloy (1.395%) showed higher wear loss (29.69 mm^3) because of its lower carbide content and reduced hardness. The study confirms that both Mo content and cooling path during destabilization heat treatment play critical roles in controlling carbide morphology, martensite stability, hardness, and ultimately the abrasive wear performance of HCCI alloys.

Keywords: High-chromium white cast iron; ASTM A532; Destabilization Heat treatment; Molybdenum; Cooling media; Abrasion resistance; Carbide precipitation; Martensite.

1. INTRODUCTION

High-chromium white cast irons (HCCI) have garnered considerable attention in material engineering due to their outstanding resistance to abrasive and erosive wear. These alloys are extensively utilized in severe service conditions such as mineral processing, cement production, coal pulverizing, and slurry transportation in the mining sector [1,2]. The critical function of components in these environments often leads to high rates of material degradation due to the combined effects of impact, friction, and abrasive particle interaction. The replacement and downtime costs associated with worn components constitute a major expenditure for these industries. Consequently, the development and optimization of wear-resistant materials like HCCI remain a priority in industrial materials research [3]. Among the various grades of wear-resistant cast irons, ASTM A532 high-chromium white cast iron stands out for its excellent wear and impact resistance. This alloy typically contains 15–30 wt.% chromium, which facilitates the formation of hard chromium carbides, Cr_7C_3, during solidification and subsequent heat treatments [4]. These carbides form as discrete particles within the microstructure and play a crucial role in resisting abrasive wear by acting as hard barriers to particle penetration and material removal. The matrix in HCCI is generally martensitic or austenitic, depending on the heat treatment, alloying elements, and cooling rate employed during processing. The martensitic matrix, in particular, provides high hardness and toughness, contributing significantly to the wear resistance of the alloy [5]. A unique attribute of HCCI is its capacity for work hardening during abrasive wear. As the softer matrix wears away, fresh, carbide-rich surfaces are exposed, thereby renewing the material's resistance to abrasion. Moreover, the presence of retained austenite in the microstructure has attracted increasing research interest. While retained austenite has historically been viewed as detrimental due to the risk of volumetric expansion and crack initiation during stress-induced transformation, emerging studies have highlighted its potential benefits in improving toughness, ductility, and transformation-induced hardening (TRIP) behavior [6,7]. Controlled amounts of retained austenite can absorb impact energy and delay crack propagation, thus enhancing wear resistance in dynamic applications. Despite the apparent advantages of combining martensite and retained austenite, there is no established consensus on the optimal proportion of retained austenite in high chromium cast irons. For instance, Liu et al. [8] reported that abrasion resistance peaked when the retained austenite content exceeded 20%, attributing this to the increased capacity for stress-induced martensitic transformation. In contrast, excessive retained austenite may result in reduced hardness and long-term dimensional instability [9]. This highlights the delicate balance between hardness, toughness, and phase stability required to optimize performance in abrasive environments.

Another critical factor influencing the microstructure and mechanical behavior of HCCI is the presence and distribution of secondary carbides, particularly those precipitated during destabilization and tempering treatments. These carbides, including both M_7C_3 and $M_{23}C_6$ types, reinforce the matrix, impede dislocation movement, and improve overall strength and wear resistance [10,11]. The destabilization heat treatment, typically conducted between 950–1050 °C, aims to dissolve austenite-stabilizing elements like carbon and chromium into the matrix, followed by controlled cooling to precipitate secondary carbides and transform retained austenite into martensite. However, the cooling rate and chemical composition, especially molybdenum (Mo) content, significantly influence this microstructural evolution. Molybdenum, in particular, is known to promote carbide formation, enhance matrix

hardenability, and improve resistance to softening during tempering [12]. Mo also contributes to the stability of martensite and the precipitation of complex carbides, which refine the microstructure and improve wear resistance. However, the interplay between Mo content, cooling media, and resultant microstructure has not been comprehensively elucidated, especially in relation to the retention of austenite, secondary carbide precipitation, and their combined effect on wear performance. Given the knowledge gaps in understanding how cooling strategies and alloying modifications affect the phase transformation kinetics and wear properties of high-chromium white cast irons, the present study is motivated to systematically investigate the role of cooling media and Mo content in tailoring microstructural features and performance. Specifically, this work aims to evaluate how varying Mo levels and different cooling paths influence the percentage of retained austenite, morphology of primary and secondary carbides, and hardness–wear resistance relationship following destabilization heat treatment. To investigate the effects of Heat treatment, three groups of samples were subjected to destabilization under varying conditions. Destabilization of high chromium cast irons typically involves heat treatment at elevated temperatures for durations of at least 4 hours [13], although some studies have reported shorter treatment times of 1 to 2 hours [14]. However, treatments lasting less than 1 hour have not yet been documented in the literature. Each experimental condition yielded three samples, which were subsequently used for data collection and detailed analysis. Destabilization of these alloys typically requires exposure to elevated temperatures for at least 4 hours [15]. However, certain studies have reported shorter durations ranging from 1 to 2 hours [16]. Notably, treatments lasting less than 1 hour have not yet been documented in the literature

The novelty of this study lies in its integrated approach to correlating microstructure, phase composition, and mechanical properties using quantitative microstructural characterization was performed using metallographic analysis and standardized abrasion testing (ASTM G65-16). Furthermore, the research explores how Mo-enriched alloys respond to air, furnace, and controlled cooling, thereby identifying conditions that offer an optimal balance between hardness and abrasion resistance. By addressing these fundamental relationships, this work provides new insights that can guide the design and heat treatment of wear-resistant alloys, enabling better performance and longer service life in aggressive industrial environments.

2. MATERIALS AND METHODS

2.1 Alloy Preparation

The high-chromium white cast iron (HCCI) alloys were produced using a medium-frequency induction melting furnace (Inductotherm Pvt. Ltd., India, capacity: 100 kg) in a commercial foundry environment. The alloys were prepared using industrial-grade charge materials consisting of steel scrap, pig iron, and ferroalloys rather than high-purity elemental materials in order to replicate practical industrial processing conditions. Ferrochrome (Fe–Cr), ferromolybdenum (Fe–Mo), ferrosilicon (Fe–Si), and ferromanganese (Fe–Mn) were added to obtain the required eutectic HCCI compositions. Three eutectic compositions containing 22–27 wt.% Cr, ~3 wt.% C, and varying Mo contents (1.20%, 1.395%, and 1.86%) were prepared.

The melting operation was carried out at approximately 1450–1500 °C to ensure complete dissolution and homogenization of alloying elements, while the molten metal was poured into prepared sand moulds at a pouring temperature of about 1400–1450 °C. To maintain the appropriate quantities of silicon and carbon, small compositional adjustments were made before pouring by adding ferrosilicon and carburizer as needed. There was no particular inoculation or melt treatment. After that, the molten metal was poured into sand molds that had already been prepared, and it was left to harden naturally. The chemical compositions, analyzed by spectrometric analysis, are listed in Table 2. All compositions conform to ASTM A532 Class III specifications.

2.2 Moulding and Casting

Moulds were prepared from silica sand bonded with resin and catalyst, then coated with zircon slurry applied manually by hand brush (Figure1 (a–b)). The molten metal was poured into preheated moulds to produce castings. After solidification, castings were shot-blasted to remove adhering sand (Figure 1 (c–e)). The Y-block casting dimensions were maintained according to ASTM A532 standards, consisting of a height of approximately 190 mm, top width of 125 mm, bottom width of 38 mm, and thickness of 50 mm to ensure controlled solidification and representative microstructural development in high-chromium white cast iron.

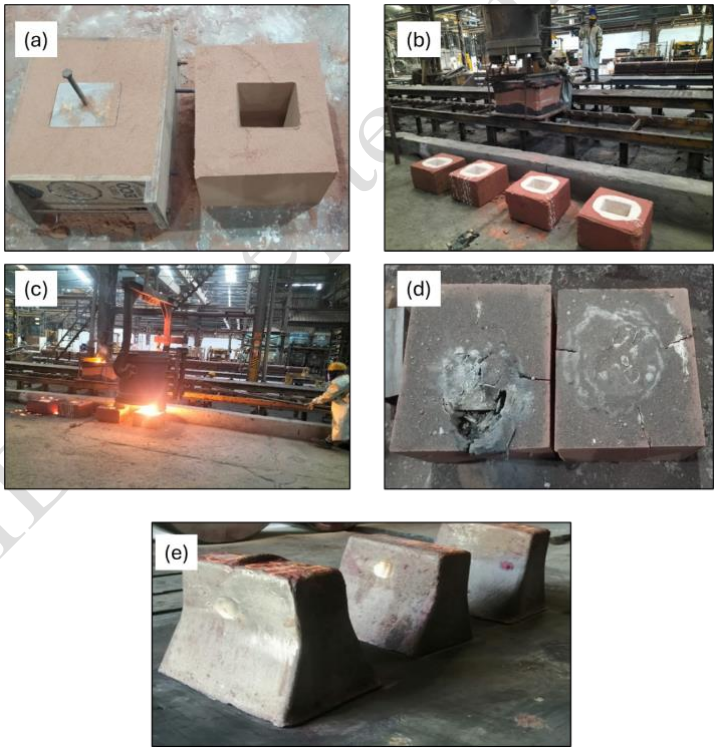

Figure 1- Fabrication sequence and geometry of the Y-block castings used in the present investigation: (a) preparation of the sand mould with Y-block cavity dimensions, (b) mould arrangement before pouring (c) molten metal pouring into the mould cavity (d) solidified Y-block castings after shakeout, and (e) ASTM A532 Y-block specimens used for heat treatment and characterization.

2.3 Heat treatment

To investigate the effects of destabilization heat treatment on the microstructure and wear performance of high-chromium white cast iron (HCCI), specimens sectioned from the central region of the ASTM A532 Y-block castings were subjected to a controlled multi-stage heat treatment cycle. The destabilization treatment was performed using a programmable resistance furnace under carefully monitored heating conditions. Prior to heating, the samples were placed in a furnace preheated to 350 °C and heated at a controlled rate of 50 °C/h up to 670 °C. Calibrated thermocouples were attached directly to the specimens to accurately monitor the internal temperature and ensure uniform heating throughout the process. The specimens were held at 670 °C for 4 h, with an additional holding time of 1 h per centimeter of volume-to-surface-area (V/A) ratio to achieve homogeneous temperature distribution and controlled destabilization within the casting section. Subsequently, the heating was continued at a rate of 40 °C/h up to 790 °C, followed by heating at 80 °C/h until the destabilization temperature of 995 °C was reached. After attaining 995 °C, the specimens were soaked for 2 h, in addition to 1 h per centimeter of V/A ratio. The soaking period was initiated only after the thermocouples confirmed that the specimen core temperature had reached the target destabilization temperature. Immediately after completion of the heat treatment cycle, the specimens were removed from the furnace and transferred to the cooling station within 2 min to avoid undesirable microstructural changes and hardness degradation. In the present investigation, the samples were cooled in still air from the destabilization temperature until ambient temperature was reached. The destabilization heat treatment promoted the precipitation of secondary carbides and transformation of the matrix into martensite during cooling, thereby enhancing hardness and abrasive wear resistance. The complete multi-stage heating schedule adopted in this study is illustrated in Table 1 and Figure 2.

Table 1: Procedure followed for the heat treatment.

Steps	Work Performed	Procedure
Step 1	Loading	Preheated furnace at 350°C (662°F)
Step 2	Holding	No holding, Treatment can start directly
Step 3	Heating up	50°C/h (90°F/h) maximum up to 670°C (1238°F
Step 4	Holding	670°C (1238°F) during 4 hours + 1h/cm V/A. The countdown starts when the casting effectively reaches that temperature.
Step 5	Heating up	40°C/h (72°F/h) maximum up to 790°C
Step 6	Heating up	80°C/h (144°F) maximum up 995°C (1904°F)
Step 7	Holding	995°C (1904°F) during 2 hours + 1h/cm V/A. The countdown starts when the casting effectively reaches that temperature.

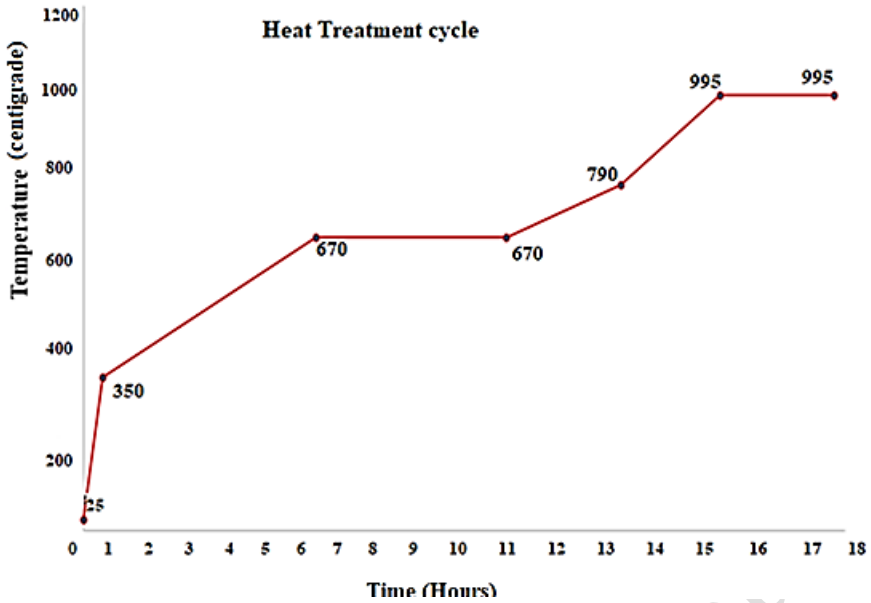

Figure 2 - The heat treatment cycle for the present study

2.4 Sample preparation

To evaluate the properties of the castings, specimens were prepared for mechanical and microstructural characterization. Specimens were prepared using an electrical discharge machining (EDM) cutter to ensure dimensional accuracy and prevent surface damage (Figure 3). Wear test specimens were prepared to dimension of 76.2 mm × 25.4 mm × 12.7 mm, as per ASTM G65 standards, while microhardness specimens were sectioned from the Y-blocks with dimensions of 50.8 mm × 50.8 mm × 50.8 mm.

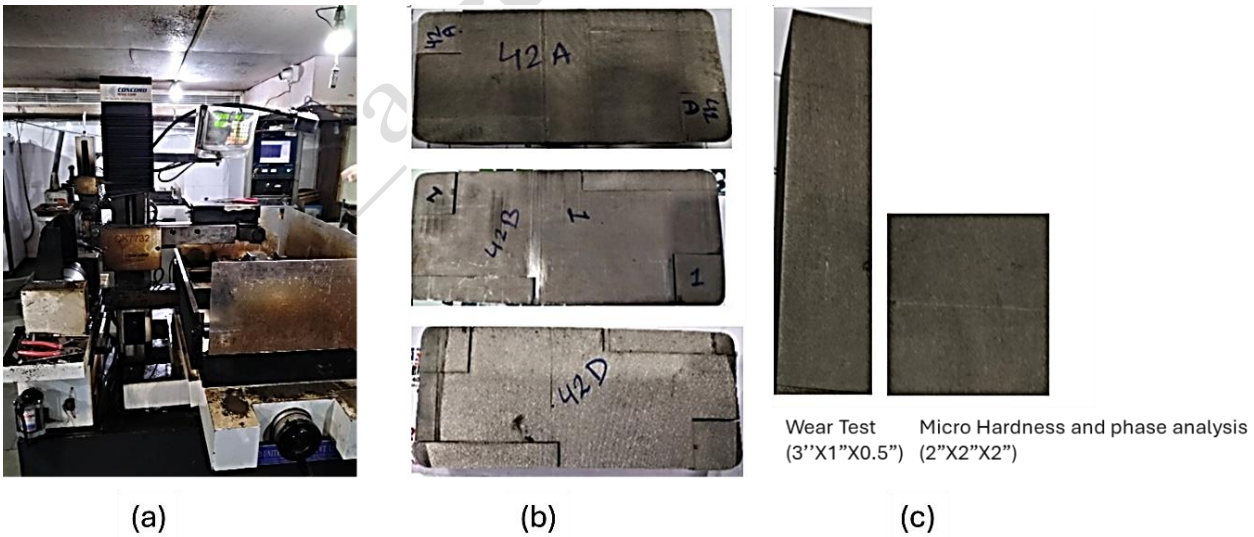

Figure 3 - (a) The EDM Cutting Machine (b) Cutting Specimen (c) The test specimens for wear test and Micro hardness and phase analysis.

2.5 Mechanical and microstructural characterization

Abrasive wear tests were performed using the rubber wheel/dry sand method according to ASTM G65-16 (Procedure A) with a normal load of 134 N, wheel speed of 120 rpm, and silica sand feed rate of 380 g/min. Mass loss was measured using an analytical balance (±0.1 mg), and wear volume was calculated from the density of the material as 7.85 g/cm³. Microhardness and macrohardness were evaluated using appropriate indentation methods. Macrohardness of the bulk samples was measured using the Rockwell hardness tester (HRC scale) with a load of 150 kgf according to ASTM E18 standards. Microhardness of the matrix and carbide phases was determined using a Vickers microhardness tester (HV0.1) with a 100 g load applied for 15 s as per ASTM E384 standards. All measurements were repeated at multiple locations, and the average values were reported. Optical microscopy was performed on polished and etched (2% Nital) samples to examine phase morphology using microstructural characterization procedure .Scanning electron microscopy coupled with energy dispersive X-ray spectroscopy (EDS) was used to identify elemental distributions within primary and secondary carbides, martensite, and retained austenite regions. Carbide volume fractions were measured by image analysis (ImageJ software) from at least 10 randomly selected fields per sample.

3. RESULTS AND DISCUSSION

3.1 Chemical analysis

The actual chemical compositions of the three alloy grades (A, B, and D) are presented in Table 2. All alloys conform to ASTM A532 Class III specifications, with chromium content ranging from 26.10% to 26.58% and carbon content between 2.97% and 3.08%. Molybdenum content was intentionally varied—1.23% (A), 1.395% (B), and 1.86% (D)—to investigate its influence on wear performance.

Table 2 : Chemical composition of Y block A, B & D.

Element (%)	Alloy A(wt.%)	Alloy B(wt.%)	Alloy D(wt.%)
C	3.06	2.97	3.08
Mn	1.15	1.15	1.845
Cr	26.58	26.53	26.1
Ni	0.23	0.31	0.249
Mo	1.23	1.395	1.86
Si	0.46	0.5	0.43
S	0.024	0.028	0.027
P	0.016	0.027	0.029
Cu	0.07	0.08	0.1
Ti	0.0279	0.0265	0.0237

3.2 Optical Microstructural Analysis

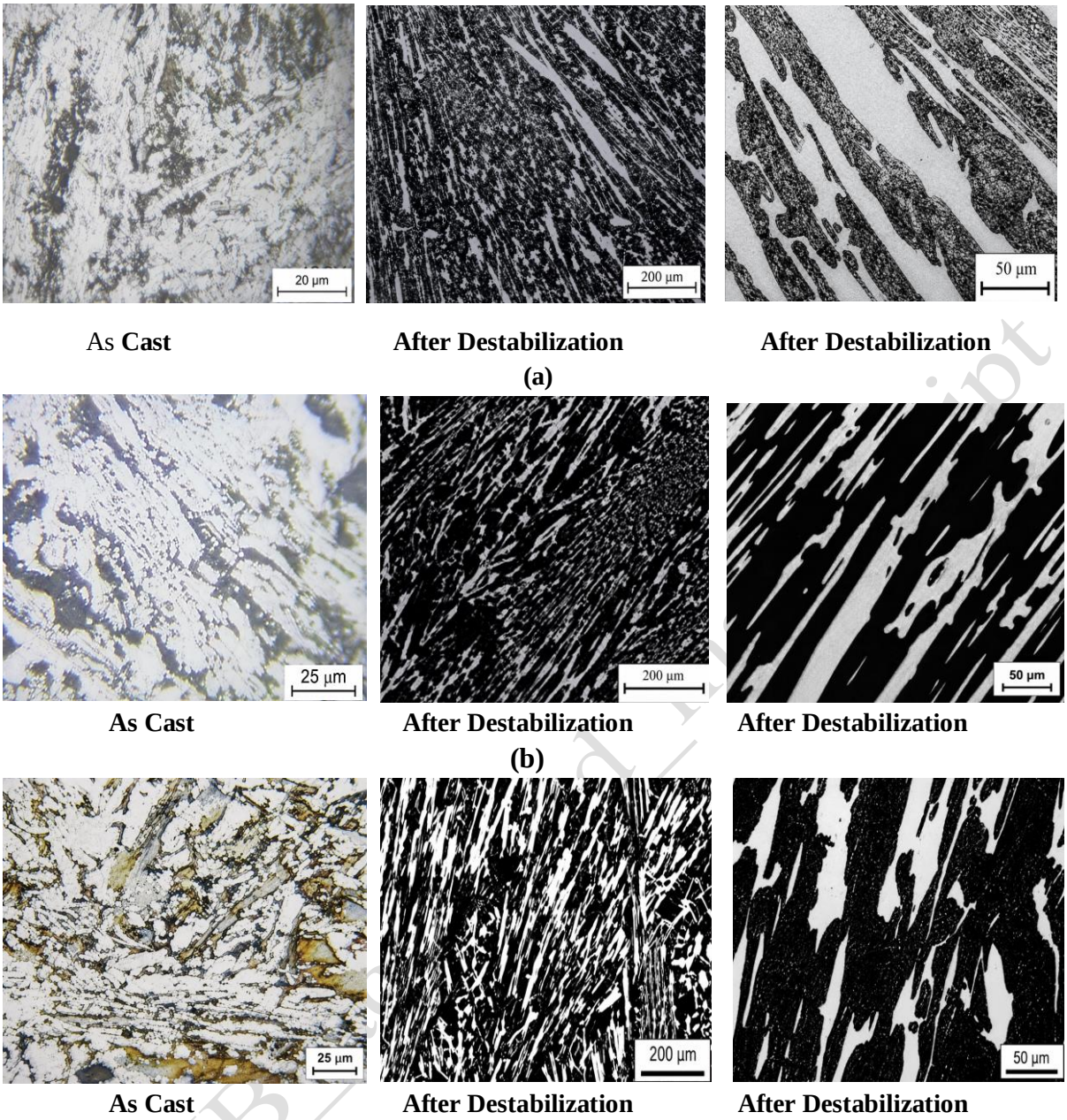

Figure 4 - Optical microstructure of (a) Y Block A, (b) Y Block B and (c) Y Block D after metallographic preparation and chemical etching

From the optical photomicrographs, the microstructures of the HCCI alloys can be clearly observed. The as-cast alloys (Y Block A, B, and D; Figure 4 (a–c)) exhibit dendritic austenite surrounded by eutectic M_7C_3 carbides, which is characteristic of their eutectic composition. After destabilization heat treatment, the matrix transformed predominantly into tempered martensite, with secondary carbides precipitating both within martensitic laths and in retained austenite regions. The measured martensite content ranged between 29–46% for Alloy A, 28–47% for Alloy B, and 27–49% for Alloy D. According to Tabrett et al. [17] and Sare & Arnold [18], martensite may also form locally adjacent to eutectic carbides, where chromium and carbon depletion raises the martensite start temperature (Ms) sufficiently to permit

transformation even under moderate cooling rates. This explains the presence of martensite across all alloys despite their high chromium content, which typically suppresses martensitic transformation. Quantitative image analysis confirmed that all alloys contained more than 30% primary eutectic M_7C_3 carbides in the as-cast state, validating their eutectic nature. Trace titanium (0.0237–0.0279%) was also detected, which has been reported to contribute to grain refinement in high-chromium irons [19].

The phase fraction analysis reveals clear trends with varying Mo content. In Alloy A (1.23% Mo), the microstructure consists of 36.59% primary carbides, 16.8% secondary carbides, and 46.62% martensite. Increasing the Mo content to 1.395% in Alloy B results in a decrease in both primary (32.95%) and secondary carbides (10.4%), while the martensite fraction rises significantly to 56.56%. However, further increasing the Mo content to 1.86% in Alloy D leads to a substantial increase in carbide fractions, with 40.72% primary carbides and 19.04% secondary carbides, while the martensite content decreases to 40.24%. These variations indicate that Mo strongly influences the balance between carbide formation and martensitic transformation. Mo is a strong carbide stabilizer. Increasing Mo promotes both primary M_7C_3 carbides and fine secondary carbides. Alloy D (1.86% Mo) exhibited the highest primary carbide fraction and the densest secondary carbide precipitation. This agrees with the findings of Albertin & Sinatora [20] and Ribeiro et al. [21], who reported that higher carbide fractions enhance wear resistance by forming a rigid skeleton that resists abrasive penetration. Moderate Mo levels improve matrix hardenability and delay carbide nucleation, allowing greater martensitic transformation, as observed in Alloy B (56.56% martensite). Similar behavior was reported by Xi et al. [22], who noted that retained austenite and martensitic transformation strongly influence toughness and wear under impact loading. However, in abrasive wear conditions, carbide morphology plays a more dominant role than martensite fraction alone. Excessive Mo (Alloy D) reduces the available matrix for martensitic transformation, lowering martensite to 40.24%. Despite this, Alloy D still achieved superior wear resistance due to the reinforcing effect of abundant carbides. This confirms observations by Sare & Arnold [23] that the balance between matrix and carbide fraction, rather than matrix hardness alone, governs wear behavior. In summary, the microstructural evolution observed in this study is consistent with earlier reports [24]. Increasing Mo shifts the balance from a martensite-dominated matrix to a carbide-reinforced microstructure. While moderate Mo favors martensite formation, higher Mo favors carbide development, and the best wear resistance occurs when a continuous carbide skeleton is present, even at the expense of lower martensite fraction. Alloy D had the highest carbide area percentage (59.76%) as shown in Table 3 and also the most uniform carbide distribution, and the shortest average carbide size (8-14µm) of all the alloys examined, according to image analysis. It is anticipated that the improved carbide network will enhance resistance to material removal and abrasive penetration.

Table 3: Quantitative Analysis of Carbide Distribution and Morphology in Destabilized High-Chromium White Cast Iron Alloys

Alloy	Primary Carbides (%)	Secondary Carbides (%)	Average Carbide Size (µm)	Mean Carbide Spacing (µm)
A	36.59	16.80	18–22	12–16
B	32.95	10.40	14–18	15–20

D	40.72	19.04	8–14	6–10

3.3 SEM and EDS Analysis

SEM observations (Figure 5) provided a finer view of the as-cast microstructures. Alloy A showed a moderately distributed eutectic carbide network, Alloy B contained coarser carbides with fewer secondary precipitates, and Alloy D displayed the densest and most refined carbide distribution. The morphology of carbides in Alloy D indicates a continuous skeleton, which has been reported to enhance abrasion resistance by forming rigid barriers against abrasive particles [25]. EDS analysis (Figure 6) confirmed the elemental distribution within these phases. The carbides were enriched in chromium and molybdenum, consistent with M_7C_3 carbides and Mo-rich complex carbides, while the matrix was primarily iron with dissolved Cr and Mo. Trace elements such as Si, Mn, and Ti were detected in small amounts, contributing to secondary effects such as deoxidation and grain refinement. These findings agree with Dogan et al. [26] and Albertin & Sinatora [27], who reported that carbide chemistry, particularly Mo enrichment, plays a crucial role in determining wear performance. Thus, SEM/EDS results support the optical microscopy and phase fraction data, showing that Alloy D developed a more continuous Mo-rich carbide skeleton, which later proved critical in enhancing wear resistance.

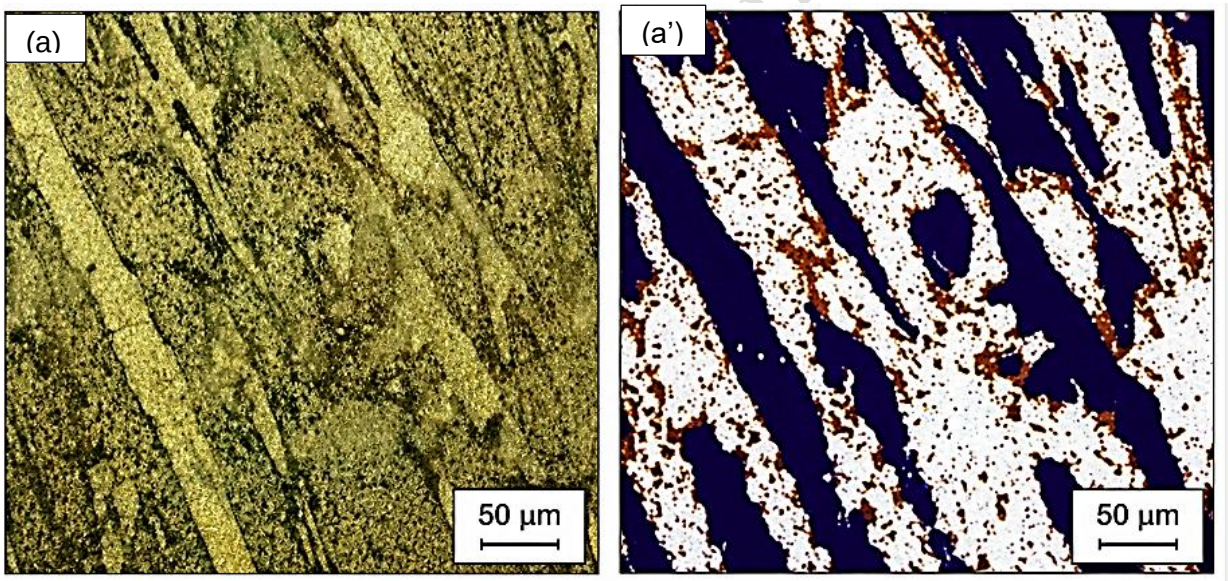

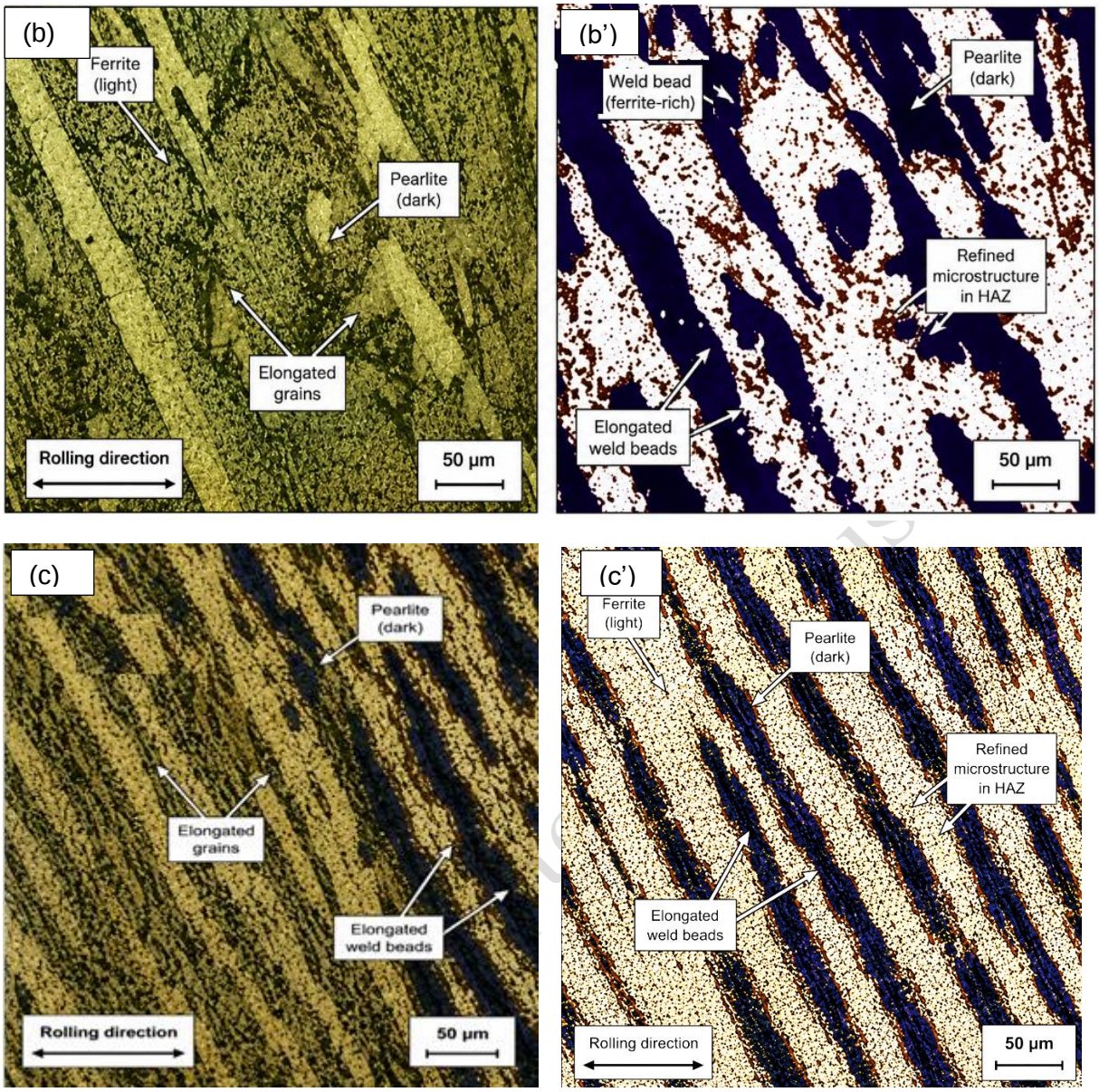

Figure 5 - SEM micrographs displaying the as-cast microstructure of high-Cr white cast iron (WCI) alloys: (a) & (a') Alloy A, (b) & (b') Alloy B, and (c) & (c') Alloy D

3.4 EDS (Energy dispersive Analysis of X-ray)

EDS Location: EDS on Surface

(a)

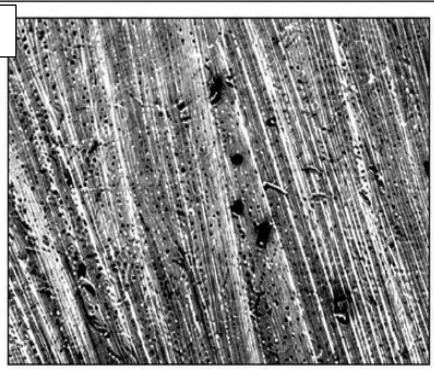

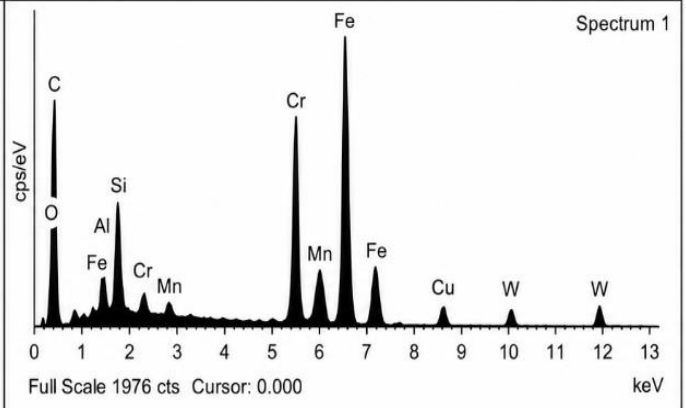

Secondary Electron Image		Energy Spectrum	
Element	**Wt. (%)**	**Element**	**Wt. (%)**
Aluminium	1.66	Silicon	1.39
Chromium	28.25	Manganese	0.97
Iron	65.73	Molybdenum	0.84
Tungsten	1.15		

EDS Location: EDS on Surface

(b

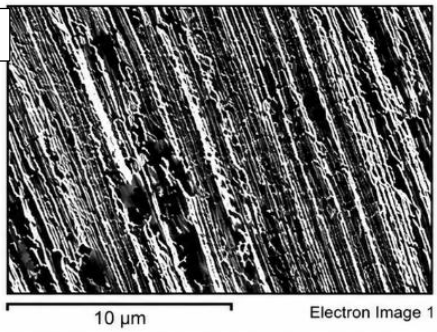

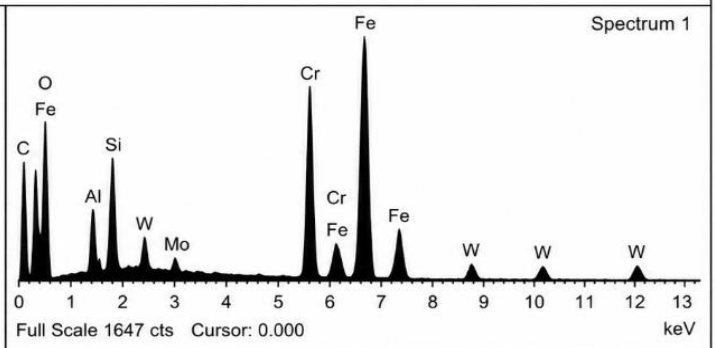

Secondary Electron Image		Energy Spectrum	
Element	**Wt. (%)**	**Element**	**Wt. (%)**
Aluminium	2.01	Silicon	0.88
Chromium	29.31	Manganese	1.63
Iron	62.23	Molybdenum	1.78
Tungsten	2.17		

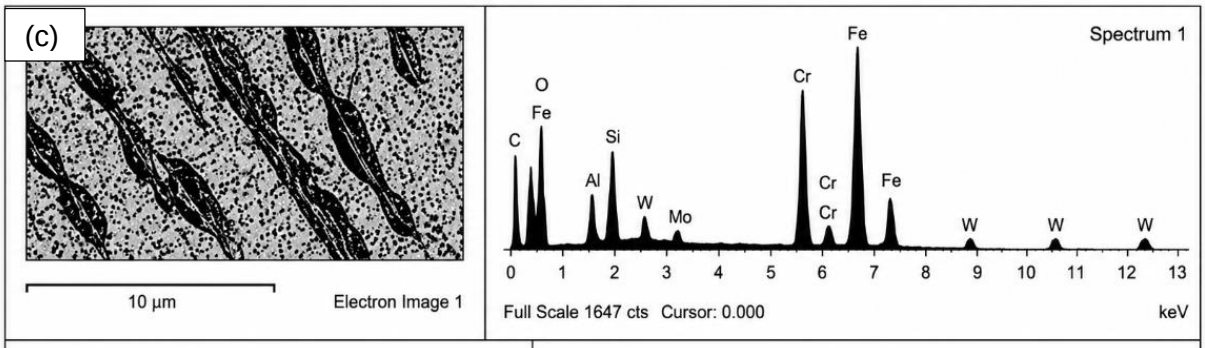

Secondary Electron Image		Energy Spectrum	
Element	**Wt. (%)**	**Element**	**Wt. (%)**
Aluminium	1.42	Silicon	0.74
Chromium	27.15	Manganese	1.28
Iron	65.38	Molybdenum	1.53
Tungsten	1.25	-	-

Figure 6 - EDS analysis on the as-cast microstructure of the alloy of high-Cr white cast iron (WCI) alloys: (a) A Forced air cooling sample, (b) B Forced Air cooling sample (c) D Still Air cooling sample

Energy Dispersive X-ray Analysis (EDX or EDS) of chromium cast iron conforming to ASTM A532, EDX provides detailed information about the distribution and concentration of elements such as Chromium, Iron, Alumunium, Tungsten, Silicon, Manganese ,Molybdenum and other alloying elements within the microstructure of sample A, sample B The results from EDX analysis provide critical insights into the material's performance, particularly its wear resistance and hardness, by showing how elements like chromium are distributed throughout the microstructure. This analysis is essential for understanding the behavior of ASTM A532 chromium cast iron in various applications, such as in mining, crushing, and milling operations where high wear resistance is required.

3.5 Wear Resistance

Wear test results (Table 4) show that Sample D (highest Mo, 1.86%) exhibited the lowest volume loss (9.03 mm^3), indicating the best wear resistance, followed closely by Sample A (1.23% Mo, 10.32 mm^3). In contrast, Sample B (1.395% Mo) showed the highest wear volume (29.69 mm^3), confirming the poorest wear resistance. Although higher carbide content generally improves abrasion resistance [28], the relationship is not strictly linear. Sample B's higher wear loss, despite a similar Cr/C ratio to Alloy A, is attributed to its lower primary carbide fraction (32.95%) and reduced secondary carbide precipitation. In contrast, Sample D's superior performance can be explained by the combination of a high primary carbide fraction (40.72%) and dense secondary carbides (19.04%), which act as hard, discontinuous barriers to abrasive particles, thereby minimizing material removal. Previous studies [29,30] have reported that retained austenite can improve impact wear resistance through the transformation-induced

plasticity (TRIP) effect. However, in this study excessive retained austenite was not observed. Instead, the results indicate that wear resistance is primarily controlled by carbide morphology and volume fraction, with matrix hardness playing a secondary role. The effect of chemical composition and microstructure on wear behavior was consistent with literature findings. The presence of hard eutectic M_7C_3 carbides improved both wear resistance and toughness, and the overall abrasion resistance of HCCI increased with carbide volume fraction [31]. This trend was evident in the current alloys: Alloy D, with the highest carbide fraction, had the best wear resistance, while Alloy B, with the lowest carbide fraction, exhibited the highest wear loss.

Table 4 : Abrasive wear test results of HCCI alloys (ASTM G65-16)

Parameter	Alloy A (1.23% Mo)	Alloy B (1.395% Mo)	Alloy D (1.86% Mo)
Test load (N)	13400	13400	13400
Wheel revolutions	2000	2000	2000
Sand flow (g/min)	380	380	380
Initial Mass (g)	151.30	153.08	150.92
Final Mass (g)	151.22	152.85	150.85
Mass loss (g)	0.08	0.23	0.07
Volume loss (mm^3)	10.19	29.29	8.91
Adjusted volume loss (mm^3)	10.32	29.69	9.03

3.6 Hardness and Phase Composition

Macrohardness testing revealed values of 63 HRC for Alloy A, 62 HRC for Alloy B, and 60 HRC for Alloy D (Table 5). Although Alloy A achieved the highest hardness, Alloy D exhibited the best wear resistance, again highlighting that hardness alone is not the primary determinant of abrasive wear performance. Phase composition analysis confirmed these trends. Alloy A had a balanced microstructure of martensite and carbides, resulting in the highest hardness. Alloy B, with the largest martensite fraction (56.56%) but the lowest carbide fraction, showed slightly lower hardness and much poorer wear resistance. Alloy D, with reduced martensite (40.24%) but abundant carbides, achieved the lowest hardness but the best wear resistance. The results of the matrix microhardness measurements were 810 ± 25 HV0.5 for Alloy A, 780 ± 20 HV0.5 for Alloy B, and 740 ± 20 HV0.5 for Alloy D. In line with its greatest macrohardness rating of 63 HRC, Alloy A displayed the highest matrix microhardness. Variations in the distribution of tempered martensite, retained austenite, and carbide precipitation within the matrix are responsible for the progressive decrease in matrix microhardness from Alloy A to Alloy D. This apparent contradiction between hardness and wear resistance has been previously discussed by Albertin et al. [32] and Hou et al. [33], who concluded that carbide fraction and morphology govern wear resistance more decisively than macrohardness in high-Cr irons. The present study

confirms this relationship: Alloy D's abundant carbide skeleton outweighed its lower hardness, delivering superior abrasion performance.

Table 5 : Hardness, wear loss, and phase composition of HCCI alloys

Property	Alloy A (1.23% Mo)	Alloy B (1.395% Mo)	Alloy D (1.86% Mo)
Macro Hardness (HRC)	63	62	60
Microhardness (HV0.5)	810 ± 25	780 ± 20	740 ± 20
Wear test (Mass loss, %)	0.08	0.23	0.07
Primary carbides (%)	36.59	32.95	40.72
Secondary carbides (%)	16.80	10.40	19.04
Tempered martensite (%)	46.62	56.56	40.24

4. CONCLUSIONS

Based on the results of the tests and examinations conducted, the following conclusions can be drawn:

1. The wear resistance of the materials is directly related to the properties of the metallic matrix and the hardness of the alloy.
2. Macro hardness values were 63 HRC (Alloy A), 62 HRC (Alloy B), and 60 HRC (Alloy D). Despite lower hardness, Alloy D showed superior wear resistance due to its higher carbide content. Increased matrix micro hardness, secondary carbide precipitation, and reduced retained austenite enhanced wear performance, confirming carbides govern abrasion resistance.
3. The thermal cycle that provided the optimal values for all examined properties involved annealing at 700°C for 6 hours, followed by destabilization at 1050°C with a soaking time of 0.5 hours.
4. When compared to the equivalent as-cast samples, the samples that were annealed before the destabilizing heat treatment showed better hardness and wear resistance. The more homogeneous microstructure created during the annealing and ensuing destabilization procedures is responsible for this improvement.
5. The destabilization heat treatment increased matrix hardness and enhanced wear resistance in high-chromium white cast irons (ASTM A532 Class III) by encouraging the precipitation of secondary carbides and decreasing the quantity of retained austenite. The observed microstructural alterations show how well the applied heat-treatment cycle improved the alloy's performance.
6. Contrary to what is commonly found in the literature and practiced in industry, the results of this study suggest that prolonged destabilization of previously annealed samples is not necessary to achieve optimal values.

REFERENCES

1. R. Sare, B.K. Arnold, G.A. Dunlop, P.G. Lloyd, Repeated impact-abrasion testing of alloy white cast irons, *Wear*, Volumes 162–164, Part B, 1993, Pages 790-801, ISSN 0043-1648, https://doi.org/10.1016/0043-1648(93)90080-6.
2. S. K. Hann and J. D. Gates A transformation toughening white cast iron", *Journal of Materials Sci Science Journal Materials Science* 32, pp 1249-1259,1997
3. H Liu, et al., "Effects of cryogenic treatment on microstructure and abrasion resistance of CrMnB high chromium cast iron subjected to sub-critical treatment", *Mater. Sci. Eng. A*, pp478, 324-328, 2008.
4. A. Kootsookos and J.D.Gates The role of secondary carbide precipitation on the fracture toughness of a reduced carbon white iron", *Material Science Engineering A490*, pp. 313-318, 2008.
5. S Yasar, Investigation of wear and microstructure of turbine pallet of sanding machine, *Institute of Science and Technology*, Gazi University, Ankara,Turkey,2001
6. G. Laird, R. Gundlach, K. Röhrig. Abrasion-resistant *Cast Iron Handbook. Ed*. American Foundry Society. Schaumburg, USA. 2000. pp. 1-222.
7. X. Jia, Q. Hao, X. Zuo, N. Chen, Y. Rong. "High hardness and toughness of white cast iron: The proposal of a novel process". *Materials Science and Engineering*. Vol. 618. 2014. pp. 96-103.
8. H. Liu, et al., Effects of deep cryogenic treatment on property of 3Cr13Mo1V1.5 high chromium cast iron", *Materials & Design* 28, pp.1059-1064, 2007.
9. Tozetti, K.D.; Albertin, E.; Scandian, C. Abrasive size and load effects on the wear of 19.9 % chromium and 2.9% carbon cast iron. *Wear* 2017, 376–377, 46–53. [CrossRef]
10. K. Zum, G. Eldis. "Abrasive Wear of White Cast Irons". *Wear*. Vol. 64. 1980. pp. 175-194.
11. Y. Hou, Y. Wang, Z. Pan, L. Yu. "Influence of rare earth nanoparticles and inoculants on performance and microstructure of high chromium cast iron". *Journal of Rare Earths*. Vol. 30. 2012. pp. 283-288.
12. E. Albertin, F. Beneduce, M. Matsumoto, I. Teixeira. "Optimizing heat treatment and wear resistance of high chromium cast irons using computationalthermodynamics". *Wear*. Vol. 271. 2011. pp. 1813-1818.
13. Y. Hou, Y. Wang, Z. Pan, L. Yu. "Influence of rare earth nanoparticles and inoculants on performance and microstructure of high chromium cast iron". *Journal of Rare Earths*. Vol. 30. 2012. pp. 283-288.
14. Ribeiroa L, Barbosab A, Vianaa F, Monteiro Baptistac A, Diasd C, Ribeiroa CA (2011) Abrasion wear behaviour of alloyed and chilled cast irons. *Wear* 270:535–540
15. Le Nué, C., Corujeira Gallo, S., Vahid, A. *et al.* Destabilization Treatment and Its Influence on Microstructure and Matrix Hardness of High-Cr Cast Iron. *Metall Mater Trans A* 54, 4952–4965 (2023). https://doi.org/10.1007/s11661-023-07216-4
16. Czerwinski F. Thermal Stability of Aluminum Alloys. *Materials (Basel)*. 2020 Aug 4;13(15):3441. doi: 10.3390/ma13153441. PMID: 32759855; PMCID: PMC7435424.
17. Tabrett, C.P., Sare, I.R., Ghomashchi, M.R. Microstructure–property relationships in high chromium white iron alloys. International Materials Reviews, Vol. 41(2), 1996, pp. 52–89.

18. Sare IR, Arnold BK (1995) The Effect of heat Treatment on the gouging abrasion resistance of alloy white cast irons. *Metall Mater Trans A* 26A:357
19. Wu, Xiaojun & Xing, Jiandong & Fu, Hanguang & Zhi, Xiaohui. (2007). Effect of titanium on the morphology of primary M 7C 3 carbides in hypereutectic high chromium white iron. Materials Science and Engineering A-structural Materials Properties Microstructure and Processing - *Mater Sci Eng A-Struct Mater*. 457. 180-185. 10.1016/j.msea.2006.12.006.
20. E. Albertin, A. Sinatora. "Effect of carbide fraction and matrix microstructure on the wear of cast iron balls tested in a laboratory ball mill". *Wear*. Vol. 250. 2001. pp. 492-501.
21. Ribeiro, L., Barbosa, A., Viana, F., Monteiro Baptista, C., Dias, C., Ribeiro, C.A. Abrasion wear behaviour of alloyed and chilled cast irons. Wear, Vol. 270, 2011, pp. 535–540.
22. Xi, J.-T.; Zhou, Q.-D.; Liu, S.-H.; Song, G.-S. Influence of retained austenite on wear resistance of high chromium cast iron under various impact loads. *Wear,* Vol. 162–164, 1993, pp. 83–88.
23. Sare, I.R., Arnold, B.K. The effect of heat treatment on the gouging abrasion resistance of alloy white cast irons. *Metallurgical and Materials Transactions A*, Vol. 26A, 1995, pp. 357–370.
24. Huan Teng, Yahui Deng, Ruibo Dang, Hongshan Zhao, Xicheng Wei, Han Dong, "Effect of carbide characteristics on abrasive wear behavior during knife honing: A comparative study of martensitic stainless steel and spring steel" , *Journal of Materials Research and Technology*, Volume 39,2025, Pages 2021-2029, ISSN 2238-7854, https://doi.org/10.1016/j.jmrt.2025.09.211.
25. Prasad, A. & Mukherjee, Subrata. (2024). A correlation between carbide morphology and wear resistance of a chromium based hard facing plate. *Sādhanā*. 49. 1-11. 10.1007/s12046-023-02409-4.
26. O. N. Dogan, J. A. Hawk and G. L. laird II, Solidification structure and abrasion resistance of high chromium white irons", *Metallurgical and Materials Transactions A* 28A, pp.1315-1328,1997.
27. Hamid Pourasiabi, J.D. Gates, Effects of chromium carbide volume fraction on high-stress abrasion performance of NbC-bearing high chromium white cast irons, *Wear*, Volumes 498–499, 2022, 204312, ISSN 0043-1648, https://doi.org/10.1016/j.wear.2022.204312.
28. Y. P.Ma, X. L. Li, D. C.Wang, X. B.Wang, S. F. Song, and X. M. Dang, "Thermodynamics and kinetics study on improving the microstructure of high chromium cast iron by multi-alloying," *Journal of Iron and Steel Research International*, vol. 19, no. S1, pp. 400–405, 2012.
29. X. Zhi, J. Xing, H. Fu, and B. Xiao, "Effect of niobium on the ascast microstructure of hypereutectic high chromium cast iron," *Materials Lett*ers, vol. 62, no. 6-7, pp. 857–860, 2008.
30. Filipovic, Mirjana & Romhanji, Endre & Kamberović, Željko. (2012). Chemical Composition and Morphology of M7C3 Eutectic Carbide in High Chromium White Cast Iron Alloyed with Vanadium. *ISIJ International*. 52. 2200-2204. 10.2355/isijinternational.52.2200.
31. Hou, Y., Wang, Y., Pan, Z., Yu, L. Influence of rare earth nanoparticles and inoculants on performance and microstructure of high chromium cast iron. *Journal of Rare Earths*, Vol. 30, 2012, pp. 283–288.